

The new improved RPCs of CMS prevailing the challenges of High-Lumi LHC

Ece Asilar*

on behalf of the CMS Muon Group

*Hanyang University,
Seoul, Republic of Korea*

E-mail: ece.asilar@cern.ch

The LHC luminosity will significantly increase in the coming years. Many of the current detectors in different subsystems need to be replaced or upgraded. The new ones should be capable not only to cope with the high particle rate, but also to provide improved time information to reduce the data ambiguity due to the expected high pileup. The CMS collaboration have shown that the new improved RPCs, using thinner gas gap with thickness 1.4 mm and low-resistivity high pressure laminate, can stand rates up to 2 kHz/cm². They are equipped with new electronics sensitive to low signal charges. This electronics was developed to read out the RPC detectors from both ends of a strip and, using timing information, to identify the position along it. The excellent relative resolution of 160 ps leads to a space resolution of 1.5 cm. The absolute time measurement determined by the RPC signals of about 500 ps will also reduce the data ambiguity due to the highly expected pileup at the Level 1 trigger. Four demonstrator chambers have just been installed in the CMS cavern. These chambers were qualified with muon beams in Gamma Irradiation Facility, located on one of the SPS beam lines at CERN. This paper presents the results of the tests performed in Gamma Irradiation Facility as well as the brand new results from commissioning of the demonstrator chambers installed at the CMS detector.

*41st International Conference on High Energy physics - ICHEP2022
6-13 July, 2022
Bologna, Italy*

*Speaker

1. Introduction

In July 2022, CMS made the world's most accurate measurement of the decay of the B_s meson into a muon pair [1]. Such measurements can only be possible with high statistics. Therefore, in the recent years, the LHC has been getting prepared for the high-luminosity period of LHC (HL-LHC). In order to cope with the high particle rate and high pileup environment of the HL-LHC, the CMS [2] MUON system has been upgraded during the second long shut down[3]. One of the important upgrade plans is the addition of the improved RPCs(iRPCs). They will be installed to the two outer stations of the CMS endcap within $1.8 < |\eta| < 2.4$ in the Endcap rings (RE3/1 and RE4/1) to extend acceptance in forward region to increase event reconstruction capabilities. The detector simulations exhibit that a muon trigger efficiency higher than 90% everywhere can be expected if iRPC hits are included in the endcap muon track finder trigger algorithm. In the next sections, the detector and its components as well as the performance results are presented.

2. The iRPC Chamber and the readout principles

Double-gap iRPC detectors with each gap made of two 1.4 mm low-resistivity High Pressure Laminate electrodes are separated by a gas gap of the same thickness. The gap active area for the iRPC RE 3/1 and RE 4/1 chambers are 12226.66 cm² and 10577.50 cm² respectively. The detectors are designed to operate in avalanche mode. A gas mixture of 95.2% $C_2H_2F_4$, 4.5% C_4H_{10} and 0.3% SF_6 has been used so far.

A trapezoidal-shape strip panel of an iRPC, sandwiched by two gas gaps, is divided into two sections in ϕ . They are 0.6-mm-thick printed circuit boards (PCB) and each contains 48 strips. Each strip has a trapezoidal shape and the pitch ranges between 0.6-1.2 cm. Figure 1 shows a schematic view of two strip PCBs.

The signal generated by a particle crossing the detector travels to two ends of the fired strip, which are defined as low (LR) and high radius (HR). The difference between the two signal arrival times $\Delta T_{(LR-HR)}$ leads to the identification of the position along the strip [4].

The new layout reduces the amount of the avalanche charge produced by the passage of a charged particle through the detector. The new front-end electronics for the iRPC (FEB v2.2) is designed to cope with the smaller charge signal of the detector, while keeping the high iRPC efficiency. Being able to achieve a threshold of 32 fC improves the rate capability. The FEB v2.2 is composed of the following components: Three 32-channel Erni connectors, 6 ASICs PETIROC [5] 2C (top & bottom), 3 FPGAs, slow control electronics. A reset function in the PETIROC-2C processor for individual channel minimises occasion of dead time on the iRPCs. In the FEB v2.2, the signals arose at the two strip ends are delivered to two different PETIROC processors. This helps to disentangle the noise and possible electronic cross-talk that can be originated from the PETIROC processors. When the amplitude of the signal is higher than the threshold of the channel, the PETIROC sends an output signal to the associated TDC channel of the FPGAs. The main task of the three FPGAs on the FEB is to time stamp the trigger signals received from the PETIROCs. The standard deviation of the $\Delta T_{(LR-HR)}$ is about 160 ps when measured with a proper time calibration after noise rejection, which corresponds to a spatial resolution of about 1.5 cm along the strip [6].

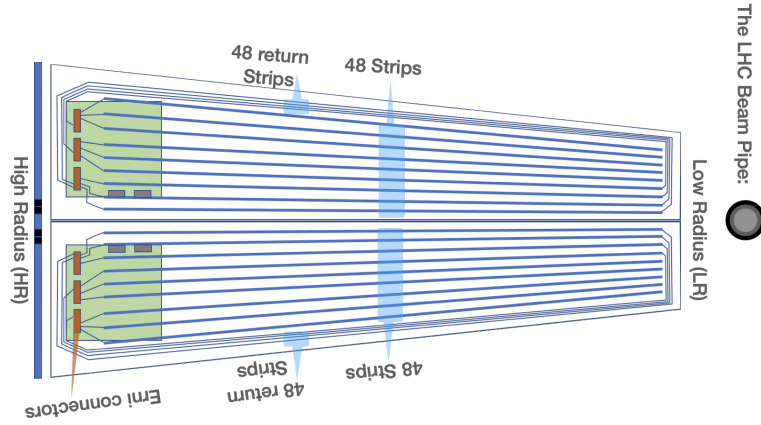


Figure 1: Schematic view of two strip PCBs and the 2 FEBs

3. Performance of iRPC detector

The iRPC detector's performance studies have been carried out in the CERN 904 Laboratory (904 Lab) [7] using cosmic muons and Gamma Irradiation Facility (GIF++) [8] located on one of the SPS beam lines of CERN. In the measurements at GIF++, the 150 GeV muon beam provided by the SPS is used as signal while gamma rays emitted from the 13 TBq ^{137}Cs source is used to emulate the LHC background. During the measurements coincidence of two plastic scintillators of a detection area of $10 \times 15 \text{ cm}^2$ are used for triggering. The presented efficiencies represent the muon trigger efficiency. In the presence of background radiation, the efficiency shown is calculated after subtraction of the estimated gamma background using events falling outside the muon window. The efficiency of the muons is calculated after a proper subtraction of the gamma background in the muon trigger-time window whose contribution is extrapolated using the gamma events lying outside the muon window. The clustering algorithm for the particle hits is carried out with the following conditions: The events have valid signals arose in the both strip ends. All strips in the same strip cluster occur within 3 ns from the fastest one.

Figure 2 shows cluster hits on the chamber. Separate colours represent data collected from different regions of the chamber. The measurement is performed at the working-point (WP) effective high voltage (HV) without the gamma background. The HV are effective values that are corrected for a pressure of 990 hPa and a temperature of 293.15 K. The WP HV is defined as $HV_{\text{knee}} + 120 \text{ V}$. HV_{knee} is defined as a HV where the efficiency reaches a 95% level of the expected maximum value. Figure 2 exhibits also successful readout in different locations of the chamber.

Figure 3 (Left) shows the efficiency in different regions of the chamber. The efficiency at the WP is $98 \pm 1\%$ everywhere on the detector. Figure 3 (Right) shows efficiency versus effective high voltage without and with background at WP. When the statistical uncertainty is smaller than 2%, the associated error bars disappear behind the data points. The single channel reset option of the PETIROC 2C was enabled during these measurements. Enabling this option allows to reduce the dead time. Hence, the drop at the plateau efficiency is less than the previous studies [9] that are done with FEBs equipped with PETIROC 2B.

Figure 4 (Left) shows the efficiencies at the WP HV as a function of the gamma background rate measured with the associated WP HV. At 0.9 kHz/cm^2 which exceeds the maximum background rate expected at the iRPCs in the HL-LHC (0.7 kHz/cm^2), the efficiency at WP HV is measured as 95%. The estimated efficiency at 2 kHz/cm^2 is about 90%. Figure 4 (Right) shows the average charge per gamma cluster as a function of the gamma background rate. The charge is calculated using the average of the currents measured for two gaps with the following formula:

$$\langle q \rangle = \frac{(I_{TOP} + I_{BOT})/2}{\text{rate}_{\gamma CLS} \cdot A_{GAP}} \quad (1)$$

where $I_{TOP}(I_{bot})$ is the current of the top (bottom) gap, $\text{rate}_{\gamma CLS}$ is the rate of gamma clusters and A_{GAP} is the area of the gap.

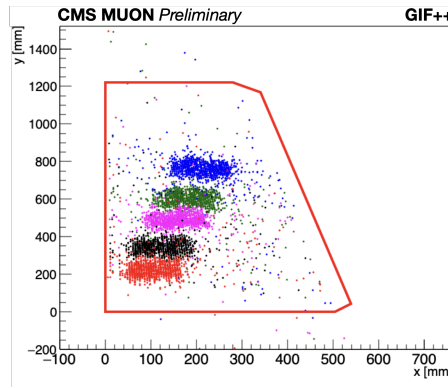


Figure 2: Cluster hits on the chamber. The effective high voltage is at the working point (WP) in the absence of background source. Separate colours represent data collected from different regions of the chamber.

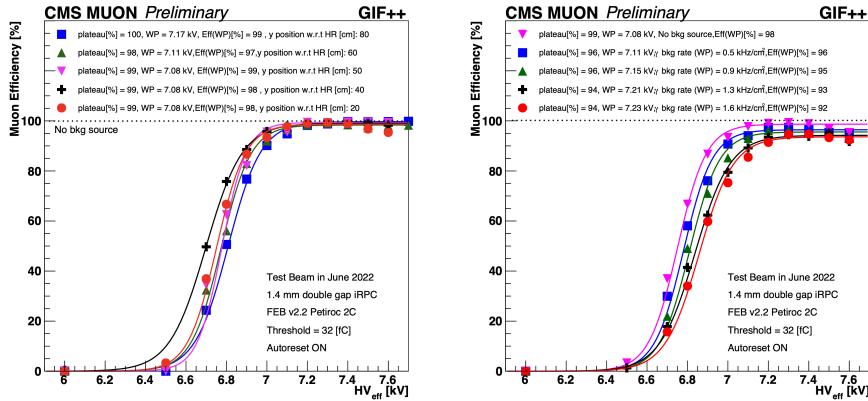


Figure 3: Left: Efficiency versus effective high voltage without background in different locations of the chamber. Right: Efficiency versus effective high voltage without and with background rates at WP.

4. Performance of the Demonstrator iRPCs at the CMS

As a result of the successful performance of the iRPC chamber and the FEB with and without background radiation, four demonstrator chambers have been installed in CMS cavern before the

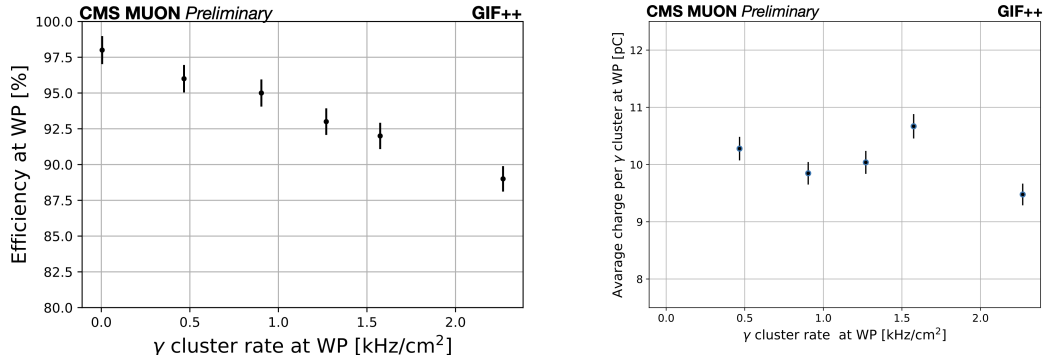


Figure 4: Left: Efficiency at working point voltage as a function of gamma background rates at the associated WP. Right: Average charge per gamma cluster at the WP versus gamma background rates at the associated WP.

start of Run 3 of the LHC. Figure 5 shows the noise distributions obtained after the installation of the chambers in CMS. A noise rate of 0.2 Hz/cm² in average and with a maximum level reaching only 1 Hz/cm² is obtained. Commissioning for the demonstrator chambers at the CMS Cavern was performed and it confirmed the stable detector operation at the temperature in the CMS-endcap closed mode with the presence of CMS endcap water cooling and with the normal magnet operation at a magnetic field of 3.8 T.

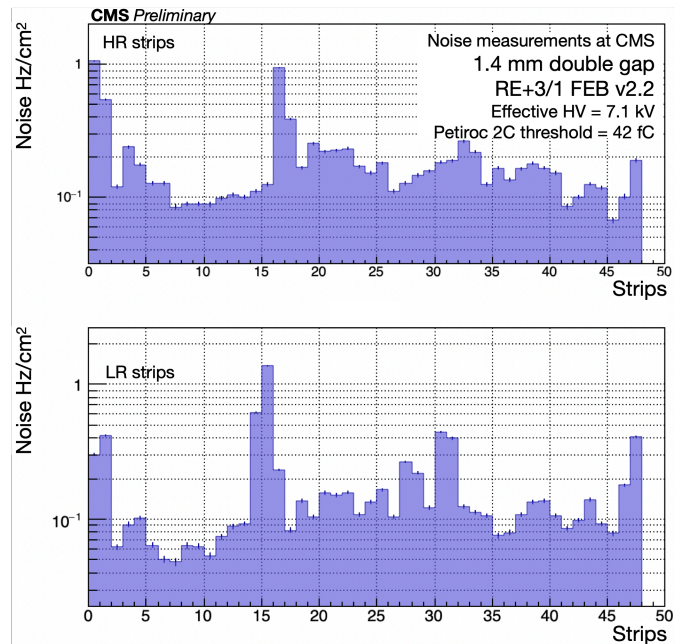


Figure 5: Figure shows the noise distributions obtained after the installation of the chambers in CMS The color filled histogram represent the number of collected hits scaled with the area of the corresponding strip and total data taking time. The upper panel of the figure shows the noise distribution of the HR strips and lower panel shows the noise distribution of the LR strips.

5. Conclusion

The new front end boards of iRPCs achieved the main goal of working with thresholds lower than 50 fC. Currently, the operating threshold is 32 fC. As a result of successful performance at CERN 904 Lab, GIF++ and at the CMS cavern, currently, demonstrator iRPCs are getting ready for taking data during Run3 to further validate the performance for HL-LHC operations. The iRPCs prevailing the challenges of HL-LHC will certainly contribute to intriguing physics program of CMS experiment.

6. Acknowledgements

We would like to acknowledge the enduring support for the Upgrade of the CMS detector and the supporting computing infrastructure provided by the following funding agencies: FWO (Belgium); CNPq, CAPES and FAPERJ (Brazil); MES and BNSF (Bulgaria); CERN; CAS, MoST, and NSFC (China); MINCIENCIAS (Colombia); CEA and CNRS/IN2P3 (France); SRNSFG (Georgia); DAE and DST (India); IPM (Iran); INFN (Italy); MSIP and NRF (Republic of Korea); BUAP, CINVESTAV, CONACYT, LNS, SEP, and UASLP-FAI (Mexico); PAEC (Pakistan); DOE and NSF (USA).

References

- [1] CMS Collaboration, Measurement of $B_s^0 \rightarrow \mu^+ \mu^-$ decay properties and search for the $B^0 \rightarrow \mu \mu$ decay in proton-proton collisions at $\sqrt{s} = 13$ TeV, .
- [2] CMS Collaboration, the cms experiment at the cern lhc, Journal of Instrumentation 3 (aug, 2008) S08004.
- [3] CMS Collaboration, The Phase-2 Upgrade of the CMS Muon Detectors, *CERN-LHCC-2017-012* (2017).
- [4] K. Shchablo, I. Laktineh, M. Gouzevitch, C. Combaret, and L. Mirabito, performance of the cms rpc upgrade using 2d fast timing readout system, Nuclear Instruments and Methods in Physics Research 958 (2020) 162139.
- [5] Petiroc, petiroc, a new front-end asic for time of flight application, IEEE Nuclear Science Symposium and Medical Imaging Conference (2013) 1–5.
- [6] H. Kou *et al.*, R&D of back-end electronics for improved resistive plate chambers for the phase 2 upgrade of the CMS end-cap muon system, Rad. Det. Tech. Meth. 6 (2022), no. 3 306–316.
- [7] E. Asilar *et al.*, performance of improved rpcs demonstrator for the cms at the hl-lhc, CMS-CR-2022-090, Preprint submitted to Nuclear Instruments and Methods in Physics Research A November (2022).
- [8] R. Guida, GIF++: The new CERN Irradiation Facility to test large-area detectors for HL-LHC, IEEE Nuclear Science Symposium and Medical Imaging Conference (2015) 1–4.
- [9] CMS Collaboration, Front-end electronics for CMS iRPC detectors, *JINST* 16 (2021) C05002.